

● *Original Contribution*

## CYCLIC CHANGES IN BLOOD ECHOGENICITY UNDER PULSATILE FLOW ARE FREQUENCY DEPENDENT

LINH CHI NGUYEN,\* FRANÇOIS T. H. YU,\* and GUY CLOUTIER\*<sup>†</sup>

\*Laboratory of Biorheology and Medical Ultrasonics, Centre hospitalier de l'Université de Montréal (CHUM)—Hôpital Notre-Dame, Montréal, Québec, Canada, and <sup>†</sup>Department of Radiology, Radio-Oncology and Nuclear Medicine, and Institute of Biomedical Engineering, Université de Montréal, Montréal, Québec, Canada

(Received 14 August 2007; in final form 4 October 2007)

**Abstract**—Previous *in vivo* and *in vitro* studies have demonstrated that blood echogenicity varies under pulsatile flow, but such changes could not always be measured at physiological stroke rates. The apparent contradiction between these studies could be a result of the use of different ultrasound frequencies. Backscattered signals from porcine blood were measured in a pulsatile Couette flow apparatus. Cyclic changes in shear rate for stroke rates of 20 to 70 beats per minute (BPM) were applied to the Couette system, and different blood samples were analyzed (normal blood and blood with hyperaggregating erythrocytes promoted with dextran). To confirm that cyclic echogenicity variations were observable, spectral analysis was performed to verify if changes in echo-amplitude corresponded to the stroke rate applied to the flow. Echogenicity was measured with two single-element transducers at 10 and 35 MHz. At 35 MHz, cyclic variations in backscatter were observed from 20 to 70 BPM. However at 10 MHz, they were detected only at 20 BPM. For all cases except for hyperaggregating red blood cells (RBCs) at 20 BPM, the magnitude of the cyclic variations were higher at 35 MHz. We conclude that cyclic variations in RBC aggregation exist at physiological stroke rates, unlike what has been demonstrated in previous *in-vitro* studies at frequencies of 10 MHz. The increased sensitivity at 35 MHz to small changes in aggregate size might be the explanation for the better characterization of RBC aggregation at high stroke rates. Our results corroborate *in-vivo* observations of cyclic blood echogenicity variations in patients using a 30-MHz intravascular ultrasound catheter. (E-mail: [guy.cloutier@umontreal.ca](mailto:guy.cloutier@umontreal.ca)) © 2008 World Federation for Ultrasound in Medicine & Biology.

**Key Words:** Red blood cell aggregation, Cyclic echogenicity variations, Pulsatile flow, High-frequency ultrasound, Backscattering coefficient.

### INTRODUCTION

Red blood cell (RBC) aggregation is a natural, reversible phenomenon that occurs in human blood vessels and plays an important role in blood flow properties. During the aggregation process, RBCs form reversible rouleaux or complex 3-D networks that result from an equilibrium between aggregating forces, such as interactions between RBCs and plasmatic macromolecules, and disaggregation forces such as the shear force of flow. Interestingly, elevated levels of RBC aggregation have been related to different circulatory pathologies, such as vascular thrombosis (Chabanel et al. 1994), coronary artery disease (Neumann et al. 1989, 1991), diabetes mellitus (Hay-

akawa and Kuzuya 1991; Le Dévéhat et al. 1996, 2000), obesity (Poggi et al. 1994; Samocha-Bonet et al. 2003), myocardial infarction and cerebrovascular accidents (Hayakawa and Kuzuya 1991; Vayá et al. 2004).

Most techniques for measuring RBC aggregation are only applicable under *in-vitro* conditions. Ultrasound imaging is a promising tool to characterize RBC aggregation because it provides real-time observations of this process *in vivo* and *in situ*. Several studies have shown that blood echogenicity is highly related to the state of RBC aggregation. They have demonstrated that echogenicity is dependent on the shear rate and on macromolecules at a sufficient concentration, such as neutral dextran and plasma fibrinogen. However, the relationship between RBC aggregation and blood echogenicity is complex because of the non-Rayleigh backscattering effect. Understanding the acoustic properties of blood is therefore necessary to characterize, *in situ*, the dynamics

Address correspondence to: Dr. Guy Cloutier, Director, Laboratory of Biorheology and Medical Ultrasonics, University of Montréal Hospital Research Center, 2099 Alexandre de Sève (Room Y-1619), Montréal, Québec, Canada, H2L 2W5. E-mail: [guy.cloutier@umontreal.ca](mailto:guy.cloutier@umontreal.ca)

of RBC aggregation and other hemorheological mechanisms that occur in blood vessels.

#### *Previous results on blood echogenicity under pulsatile flow*

Few studies have characterized RBC aggregation *in vivo* and *in situ*. De Kroon *et al.* (1991) were the first to report *in-vivo* cyclic variations of blood echogenicity by using a 30-MHz intravascular ultrasound device. The catheter was placed in the iliac artery of patients with coronary artery disease and cyclic changes in blood echo-density were measured. They suggested that the echo-density variations were associated with changes in the state of RBC aggregation related to the flow rate increase and decrease during a cardiac cycle. Concurrently and following this *in-vivo* investigation, several *in-vitro* studies have been performed with porcine blood in pulsatile mock flow by using 10-MHz Doppler transducers. However, no cyclic variation of blood echogenicity was evident from these *in-vitro* results under physiological stroke rates. Cloutier and Shung (1991, 1993) discerned cyclic changes in Doppler power at 20 beats per minute (BPM), but no variation was apparent at 70 BPM. Moreover, Wu and Shung (1996) and Lin and Shung (1999) also demonstrated that cyclic changes in Doppler power existed only at low pulsatility. Other studies have examined the effect of acceleration during systole on RBC aggregation and found no obvious variations of echogenicity at 60 BPM (Paeng *et al.* 2001; Paeng and Shung 2003). To explain the absence of cyclic variations in blood echogenicity at high stroke rates, these authors suggested that RBCs do not have time to aggregate or disaggregate during the different phases of the flow cycle.

The apparent contradiction between *in-vivo* and *in-vitro* studies at physiological stroke rates could be related to the use of different ultrasound frequencies or characteristics. Thus, our hypothesis is that high-frequency transducers might have an improved detection to small RBC aggregate size variations at high stroke rates and could outperform low-frequency transducers for this application. Another hypothesis that might explain differences between *in-vivo* and *in-vitro* results is that blood from patients with coronary artery disease, as studied by De Kroon *et al.* (1991), is likely more prone to be hyperaggregating than porcine blood. Consequently, RBC aggregation and disaggregation at high stroke rates might occur with pathologic blood because of the higher aggregation kinetics and larger size of RBC clusters.

#### *Objectives of the present study*

The focus was to compare cyclic variations of blood echogenicity obtained with high-frequency (35 MHz) and lower-frequency (10 MHz) transducers. It also ex-

Table 1. Description of studied blood samples

Name	Acronym	Hematocrit (%)	Suspending medium
Total blood	TH40	40	Plasma
Dextran blood	DH40	40	Isotonic saline water with dextran 512 kDa at 30 g/L
H6 suspension	H6	6	Isotonic saline water

amined the effect of stroke rate and different blood types (normal and hyperaggregating RBCs) on echogenicity under pulsatile flow.

## MATERIALS AND METHODS

### *Blood preparation*

Because porcine blood is known to have similar RBC aggregation properties to normal human blood (Weng *et al.* 1996), it was used in this study. Fresh porcine blood was collected from a local slaughterhouse and anticoagulated with 3 g/L of ethylene diamine tetra acetic acid (EDTA). Then, blood samples were centrifuged for 15 min at 3,000 RPM (1,855g) at room temperature, the buffy coat layer containing white cells and platelets was removed, the plasma was separated from RBCs and replaced with isotonic saline solution for a second centrifugation, and then three 70-mL blood samples were prepared as described in Table 1.

The TH40 was referred to normal blood, whereas DH40 corresponded to hyperaggregating RBCs (Boynard and Lelievre 1990; Meiselman 1993). The DH40 samples were prepared by mixing washed RBCs with a dextran 512 kDa saline solution. The dextran powder (lot 124H0055, Sigma Chemical, St. Louis, MO, USA) was dissolved into saline at a concentration of 30 g/L of solution. The TH40 and DH40 samples were studied for the kinetics of RBC aggregation under pulsatile flow. The H6 suspension was used as a reference medium (nonaggregating Rayleigh suspension) for signal normalization (see Signal processing). All hematocrits were measured by microcentrifugation. Experiments were performed within 48 h of blood collection.

### *Pulsatile Couette flow system*

The acoustic properties of blood were measured in a Couette flow system illustrated in Fig. 1. The rotating inner cylinder had an external diameter of 160 mm, and the stationary outer cylinder had an internal diameter of 164 mm. The rotating cylinder was attached to a stepper motor driven by a controller (Zeta 6104, Compumotor, Rohnert Park, CA, USA). Unlike Poiseuille tube flow, the shear rate in a Couette apparatus is spatially homogeneous within the 2-mm gap, for the design of Fig. 1, separating the two cylinders. Consequently, this set-up

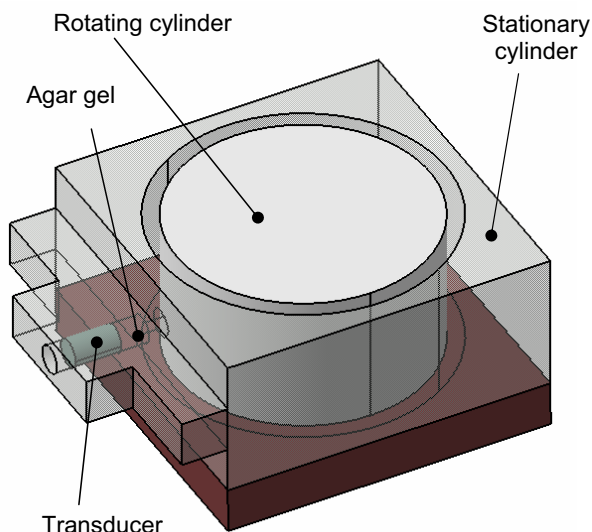


Fig. 1. Couette flow system for blood echogenicity measurements.

was ideal to precisely modulate the shear rate-dependent RBC aggregation process. The blood sample was introduced between the two concentric cylinders and submitted to cyclic variations in shear rate. Figure 2 shows the cyclic variations in shear rate applied to blood samples. For each aggregation kinetics, a shear rate of  $500 \text{ s}^{-1}$  was first applied for 35 s to attain an initial disaggregated state. Then, the shear rate was changed from  $2 \text{ s}^{-1}$  during diastole to  $100 \text{ s}^{-1}$  during systole at stroke rates of 20, 45 and 70 BPM, with a duty cycle of 10%. The duty cycle was defined as the ratio between systolic time and the duration of one pulsatile cycle. The time origin of zero was set after 35 s, when cyclic variations in shear rate started to be applied. The H6 suspension was also sheared in the Couette system at  $50 \text{ s}^{-1}$  for reference measurements. The Couette flow system was housed in a chamber and maintained at a constant temperature of  $37^\circ \text{ C}$ .

#### Ultrasound recordings

Two single-element transducers were used to compare the backscattering properties of blood: a 35-MHz center frequency-focused transducer, with a  $-6 \text{ dB}$  bandwidth from 28 MHz to 45 MHz (model PVDF 054-40-6, Visualsonics, Toronto, Ontario, Canada) and a 10-MHz center-frequency plane transducer, with a  $-6 \text{ dB}$  bandwidth from 9 MHz to 14 MHz (V312-SU, Panametrics, Waltham, MA, USA). Both transducers were positioned at 90 degrees with respect to the flow. The 35-MHz transducer with a 3-mm diameter was positioned for measurements at the center of the co-axial cylinder gap, at its focal length (6 mm), whereas the 10-MHz transducer with a 6-mm diameter was adjusted for re-

cordings at 15 mm. A gel obtained by mixing agar powder at a concentration of 30 g per liter into a 8 mL/100 mL glycerol/distilled water mixture, served as a coupling medium between the transducer and the blood sample. The solidified gel filling the transducer cavity was also useful to avoid any blood flow disturbance in the Couette system (Fig. 1).

The pulse-echo acquisition system consisted of an Avtech pulse generator (AVB2-TA-C-CRIMA, Ottawa, Ontario, Canada), a Ritec diplexer (RDX-6, Warwick, RI, USA), a 10-dB Mitec linear amplifier (model AU-A3-0120, Hauppauge, NY, USA), and a Panametrics pulser receiver (5900 PR, Waltham, MA, USA) that was used for further amplification and bandpass filtering. The radiofrequency (RF) acoustic signals were digitized with an 8-bits Gagescope acquisition board (8500CS, Montreal, Quebec, Canada) at a sampling frequency of 500 MHz. The RF signals were recorded from the test samples (TH40 and DH40), the H6 suspension and from a plane reflector used for calibration (see Signal processing). For the kinetic experiments, three RF lines were recorded every 0.1 s starting at  $t = 0 \text{ s}$  (see Fig. 2), when cyclic variations in shear rate were applied to the flow. Every kinetics was then repeated 20 times for each stroke rate to increase the signal-to-noise ratio (SNR) of any given experiment. All measurements were averaged over five TH40 and five DH40 blood samples collected from different animals. A minimum of 10 cycles were recorded for every kinetic measurement. For the plane reflector and the H6 suspension stirred in a beaker, 100 consecutive RF lines were acquired, whereas 20 RF lines were recorded for the H6 suspension placed in the Couette setup. The H6 suspensions within the beaker were used in eqn (1), whereas the H6 suspensions within the Couette apparatus were utilized in eqn (2) given below.

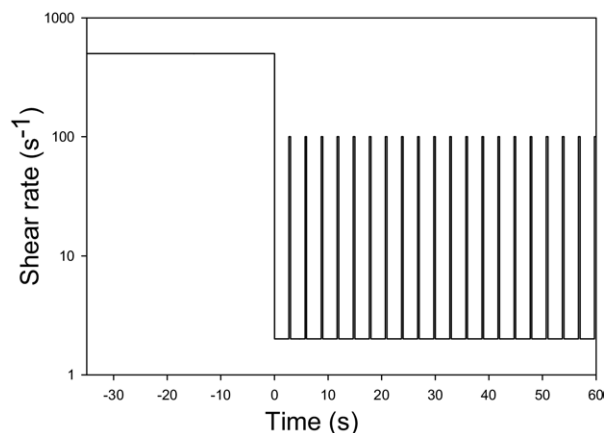


Fig. 2. Shear rate pattern applied to each blood sample to initially disaggregate RBCs and then induce pulsatile flow. This example is for a stroke rate of 20 BPM.

### Signal processing

The backscattering coefficient of blood ( $BSC_{blood}$ ) was calculated according to the modified substitution method, as in Yu and Cloutier's (2007) work using eqn (1):

$$BSC_{blood} = BSC_{H6} \times \frac{S_{blood}}{S_{H6,1}} \times \exp(4d(\alpha_{blood} - \alpha_{H6})) \quad (1)$$

Here,  $BSC_{H6}$  is the BSC of the H6 reference suspension in a beaker computed using eqn (2).  $S_{blood}$  and  $S_{H6,1}$  are, respectively, the power spectrum of the backscattered signal from the test sample and from the H6 medium measured in the Couette system. The parameters  $d$ ,  $\alpha_{blood}$  and  $\alpha_{H6}$  are the inspected depth, attenuation coefficients of blood and of the H6 medium, respectively. The values of  $\alpha_{blood}$  and  $\alpha_{H6}$  were approximated at 0.22 dB/cm/MHz (Greenleaf 1986) for blood and 0.03 dB/cm/MHz (Wang and Shung 1997) for the H6 medium.  $BSC_{H6}$  was computed as:

$BSC_{H6}$

$$= \frac{S_{H6,2}}{S_{plane}} \times \frac{1}{0.63^2} \times \frac{Rp^2k^2a^2}{8\pi d \left(1 + \left(\frac{ka^2}{4d}\right)^2\right)} \times \exp(4\alpha_{H6}d) \quad (2)$$

where  $S_{H6,2}$  is the H6 suspension stirred in a beaker with a magnetic agitator to avoid sedimentation and  $S_{plane}$  is the power spectrum of the reflected signal from a stainless steel plane submerged in distilled water. Variables  $R_p$ ,  $k$  and  $a$ , respectively, represent the reflection coefficient from the planar reflector (assumed to be 1), the wave number and the transducer radius. For each medium, the power spectrum was windowed at 1,024 points, zero padded to 2,048 points, fast Fourier transformed (FFT) and then averaged over the RF lines to provide a mean power spectrum.

### Fitting of the aggregation kinetic curves

The aggregation kinetics were characterized by computing the relative BSC ( $\Delta BSC$ ) in dB, which allowed comparisons between both transducers. The absolute BSC was first calculated from eqn (1) and expressed in  $\text{cm}^{-1}\text{sr}^{-1}$ . For each transducer, the absolute BSC after applying a shear rate of  $500 \text{ s}^{-1}$ , which corresponds to an initial disaggregated state (at  $t = 0 \text{ s}$ ), was set at the 0-dB reference. We then modeled the temporal evolution of  $\Delta BSC$  with a sigmoid curve (Fig. 3), as in the work of Rouffiac *et al.* (2002). As seen on this figure, the sigmoid curve has two distinctive zones, a transition regime (TR) and a permanent regime (PR). The sigmoid was fitted on the mean  $\Delta BSC$  and therefore ignored the cyclic echogenicity variations within PR. The sigmoid in Fig. 3 was defined by the following equation:

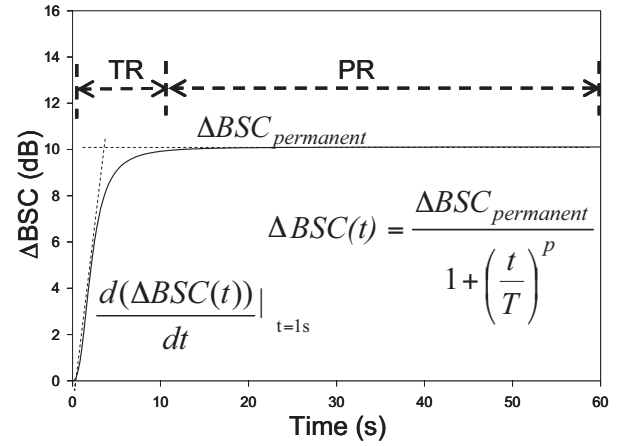


Fig. 3. Aggregation kinetic modeling using a sigmoid fitting. Two parameters are obtained from the fitting:  $\Delta BSC_{permanent}$  and the aggregation kinetic slope computed from the derivative of the sigmoid curve at  $t = 1 \text{ s}$ . Two regimes are defined on this figure, a transition regime (TR) and a permanent regime (PR).

$$\Delta BSC_{blood}(t) = \frac{\Delta BSC_{permanent}}{1 + \left(\frac{t}{T}\right)^p} \quad (3)$$

where  $\Delta BSC_{permanent}$ ,  $t$ ,  $T$  and  $p$  are, respectively, the  $\Delta BSC_{blood}$  reached during the permanent regime, the time and two constants obtained from the sigmoid fitting.  $\Delta BSC_{permanent}$ ,  $T$  and  $p$  were solved by least mean-squared fitting with Sigma Plot 2000 (v. 6.00, Systat Software, San Jose, CA, USA). Two parameters from eqn (3) were used to compare the aggregation kinetics:  $\Delta BSC_{permanent}$  and the aggregation kinetic slope computed from the derivative of eqn (3) at  $t = 1 \text{ s}$ .  $\Delta BSC_{permanent}$  and the aggregation kinetic slope allowed comparison of the transducer sensitivity to RBC aggregation.  $\Delta BSC_{permanent}$  is an index that is determined by the mean aggregate sizes and non-Rayleigh backscattering behavior, whereas the aggregation kinetic slope is a measure of the blood sample "aggregability" from a disaggregated state.

### Computation of the mean cyclic variations in echogenicity

Within PR, BSC averaging was performed over the last 10 cycles from five different experiments ( $n = 50$ ) by registering the maxima of a fitted sinusoidal function at known pulse rates of 20, 45 or 70 BPM, depending on the stroke rate applied to the flow. To improve averaging at high stroke rates, oversampling of the data was performed by convolving the zero-padded data with a sine cardinal. The data were interpolated by double oversampling at 45 BPM (double zero padding) and triple oversampling at 70 BPM (triple zero padding).

Spectral analysis was performed to confirm that cyclic variations of  $BSC_{blood}$  were not artifactual and

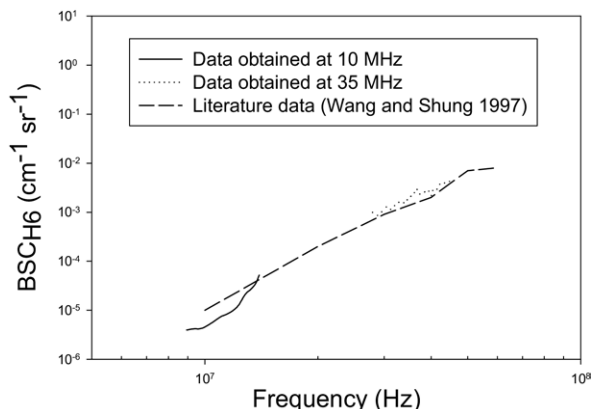


Fig. 4. Backscattering coefficient of the H6 suspension ( $BSC_{H6}$ ) and comparison with the literature (Wang and Shung 1997), showing Rayleigh scattering behavior ( $BSC \sim f^4$ ).

therefore related to cyclic changes in shear rate. Variations of echogenicity were considered observable if the main frequency component (frequency with the highest magnitude) of the FFT spectrum corresponded to the stroke rate.

Statistical analysis

Three-way analyses of variance (ANOVA, Sigma-Stat, v. 3.11, Systat) with the Tukey test for multiple comparisons were performed to compare the effect of the transducer, blood type and stroke rate. These statistical tests were conducted on  $\Delta BSC_{permanent}$ , aggregation kinetic slopes, and cyclic variations of BSC. A significance level of  $p < 0.05$  was considered to be statistically significant.

RESULTS

H6 data

To validate the modified substitution method described by eqns (1) and (2), we compared in Fig. 4 our  $BSC_{H6}$  data with previous results from the literature (Wang and Shung 1997). These authors had shown that Rayleigh behavior ( $BSC \sim f^4$ ) was respected at a low hematocrit for frequencies up to 30 MHz. It can be seen that our  $BSC_{H6}$  is comparable to these results.

RBC aggregation kinetics

Examples of aggregation kinetics under pulsatile flow are presented in Fig. 5. Figures 6 and 7 report the  $\Delta BSC_{permanent}$  and aggregation kinetic slope values obtained by the sigmoid fitting of eqn (3). ANOVA tests confirmed that the  $\Delta BSC_{permanent}$  (Fig. 6) and the aggregation slope (Fig. 7) were significantly higher at 35 MHz than at 10 MHz ( $p < 0.001$ ). Also,  $\Delta BSC_{permanent}$  for DH40 samples were significantly higher than TH40 ( $p <$

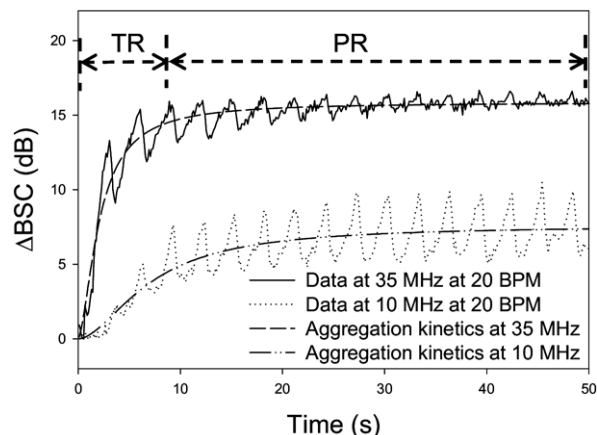


Fig. 5. Aggregation kinetics of hyperaggregating RBCs under pulsatile flow at 20 BPM obtained with the 35-MHz and 10-MHz transducers. Two regimes are identified on this figure, a transition (TR) and a permanent (PR) regimes.

0.001), for all stroke rates. For the aggregation kinetic slope, DH40 samples had higher values than TH40 ( $p < 0.001$ ) at 35 MHz only, for all stroke rates. Finally, the stroke rate did not have a significant effect on both  $\Delta BSC_{permanent}$  ( $p = 0.103$ , Fig. 6) and the aggregation slope ( $p = 0.675$ , Fig. 7).

Cyclic variations of blood echogenicity

Cyclic changes of BSC during the PR phase are presented in Figs. 8 and 9 for stroke rates of 20 and 70 BPM. The mean value of BSC was set to 0 dB. To

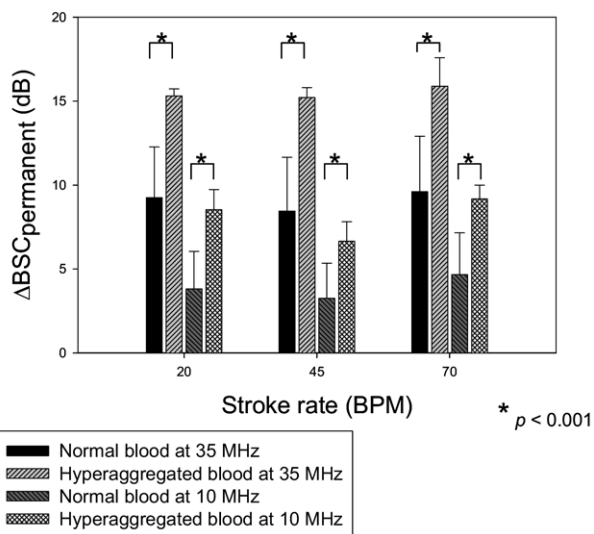


Fig. 6. Relative backscattering coefficient in PR ( $\Delta BSC_{permanent}$ ) obtained at 35 MHz and 10 MHz for normal blood and hyperaggregating RBCs. Each result represents the mean  $\pm$  one standard deviation computed over five experiments.

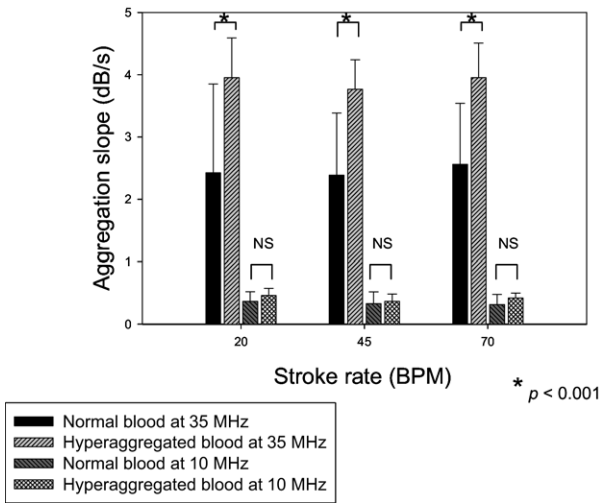


Fig. 7. Aggregation kinetic slope obtained at 35 MHz and 10 MHz for normal blood and hyperaggregating RBCs. Each result represents the mean  $\pm$  one standard deviation computed over five experiments.

verify if these cyclic variations were not artifactual, Figs. 10 (20 BPM) and 11 (70 BPM) show mean spectrograms of BSC for five pulsatile cycles within the PR phase that were averaged over five experiments. The standard deviations are not shown on spectrograms for clarity.

Cyclic variations were reliable if the main frequency component corresponded to the stroke rate applied to the flow. For a pulsatile flow at 20 BPM, the

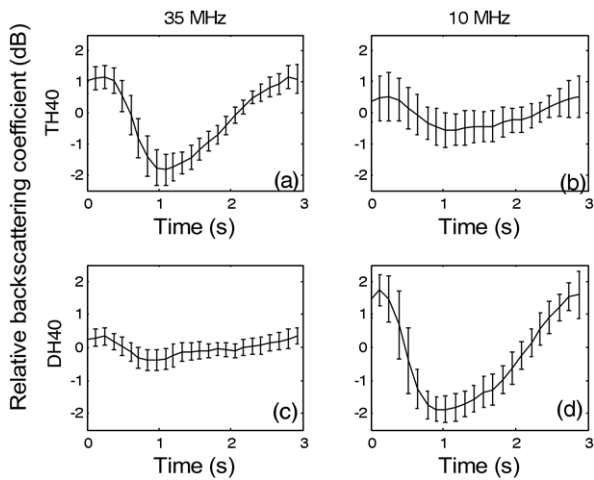


Fig. 8. Variations of the relative backscattering coefficient at a stroke rate of 20 BPM. (a, b) At 35 and 10 MHz, respectively, with normal blood samples, and (c, d) at the same frequencies with hyperaggregating RBCs. Each result represents the mean  $\pm$  one standard deviation computed over 50 cycles from five experiments.

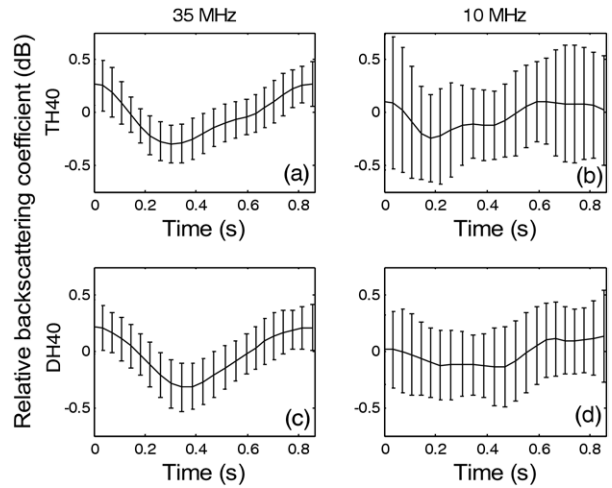


Fig. 9. Variations of the relative backscattering coefficient at a stroke rate of 70 BPM. (a, b) At 35 and 10 MHz, respectively, with normal blood samples, and (c, d) at the same frequencies with hyperaggregating RBCs. Each result represents the mean  $\pm$  one standard deviation computed over 50 cycles from five experiments.

main frequency component was observed at 0.33 Hz (20 BPM) for both transducers and both blood types (Fig. 10). At 70 BPM, the main frequency component corresponded to 1.2 Hz (70 BPM) at 35 MHz (Fig. 11a, c), but this was not the case at 10 MHz (0.24 Hz, 14 BPM, Fig. 11b, d). Therefore, at 10 MHz and 70 BPM, the cyclic variations reported in Fig. 9b and d are artifactual. Table 2 summarizes values of the mean cyclic BSC changes in dB at all stroke rates and the main frequency component

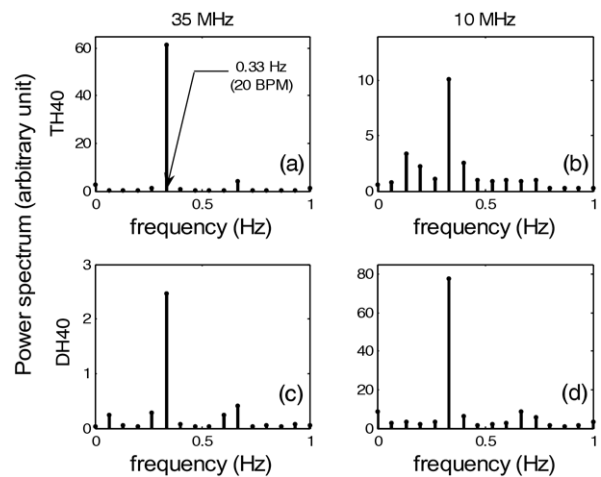


Fig. 10. Mean spectrograms of the  $\Delta$ BSC for five pulsatile cycles at 20 BPM. (a, b) At 35 and 10 MHz, respectively, with normal blood samples, and (c, d) at the same frequencies with hyperaggregating RBCs. Each result was averaged for five pulsatile cycles and five experiments.

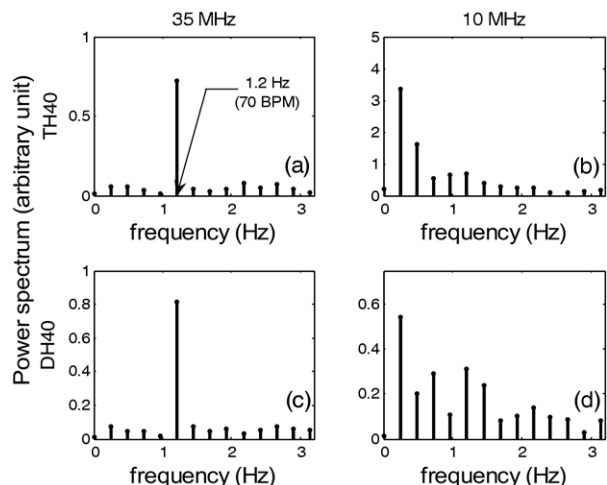


Fig. 11. Mean spectrograms of the  $\Delta BSC$  for five pulsatile cycles at 70 BPM. (a, b) At 35 and 10 MHz, respectively, with normal blood samples, and (c, d) at the same frequencies with hyperaggregating RBCs. Each result was averaged for five pulsatile cycles and five experiments.

of the cyclic variations for both transducers and blood types. The three-way ANOVA revealed that the stroke rate and transducer’s frequency had a significant effect on cyclic variations of BSC ( $p < 0.001$ ) but not the blood type ( $p = 0.509$ ). More specifically, cyclic variations decreased with increasing stroke rate, except for DH40 at 35 MHz, where variations at 20 BPM were not significantly different from those at 70 BPM.

**DISCUSSION**

*Measurements of the aggregation kinetics*

*Effect of the transducer.* As shown in Figs. 6 and 7, the 35-MHz transducer provided significantly higher val-

ues of  $\Delta BSC_{permanent}$  and aggregation kinetic slope than the 10-MHz probe for both TH40 and DH40 bloods. After a disaggregation phase at  $500\text{ s}^{-1}$ , the flow was reduced to a mean shear rate of  $11.8\text{ s}^{-1}$  ( $100\text{ s}^{-1}$  during the mimicked systole and  $2\text{ s}^{-1}$  during diastole with a duty cycle of 10%). To explain and confirm the sensitivity difference to aggregation between both transducers, we performed complementary experiments at a constant step shear rate change (*i.e.*, no pulsatility, see Fig. 12a and b). A shear rate of  $100\text{ s}^{-1}$  was first applied, as for the mimicked systole, followed by the phase of aggregation kinetic at a constant shear rate of  $2\text{ s}^{-1}$ , which corresponds to the mimicked diastolic shear rate of our pulsatile flow experiments. Note that a second objective of these other measures was to prove that the higher  $\Delta BSC_{permanent}$  and aggregation kinetic slope at 35 MHz (focused probe) could not be attributed to the fact that measurements at 10 MHz were performed with a nonfocused transducer. Additional recordings were thus realized with a focalized-10 MHz probe (model V312-SM, Panametrics), as shown in Fig. 12b.

According to this figure (panel b), focusing of the 10-MHz transducer does not modify the aggregation kinetic profile. However, Fig. 12a and b shows that aggregation kinetics differ considerably between 35 MHz and 10 MHz transducers, and between TH40 and DH40 bloods. In Fig. 12a with normal RBCs, only one zone exists with  $\Delta BSC$  higher at 35 MHz (zone 1a). In Fig. 12b with hyperaggregating RBCs, two zones can be observed: a first one where  $\Delta BSC$  are higher at 35 MHz (zone 1b), and a second one with  $\Delta BSC$  higher at 10 MHz (zone 2). The existence of higher  $\Delta BSC$  at 10 MHz (zone 2) is well known from the literature, and an explanation is the existence of non-Rayleigh backscattering at 35 MHz that reduces the intensity of echoes when

Table 2. Cyclic variation of the backscattering coefficient for normal blood (TH40) and hyperaggregating RBCs (DH40) at 35 MHz and 10 MHz, for different stroke rates

Blood sample	Stroke rate (BPM)	Transducer (MHz)	Main frequency component (BPM)	Cyclic variation (dB)
TH40	20	35	20	$3.0 \pm 0.8$
		10	20	$1.1 \pm 1.3$
	45	35	45	$1.1 \pm 0.3$
		10	18	Not observable
DH40	20	35	70	$0.6 \pm 0.3$
		10	14	Not observable
	45	35	20	$0.7 \pm 0.5$
		10	20	$3.6 \pm 0.6$
70	35	45	$1.0 \pm 0.3$	
	10	9	Not observable	
		35	70	$0.5 \pm 0.4$
		10	14	Not observable

Each cyclic variation value represents the mean  $\pm$  one standard deviation computed over 50 cycles from five experiments. Each pair of multiple comparisons were significantly different ( $p < 0.002$ ) except for those indicated by NS (non-significant).

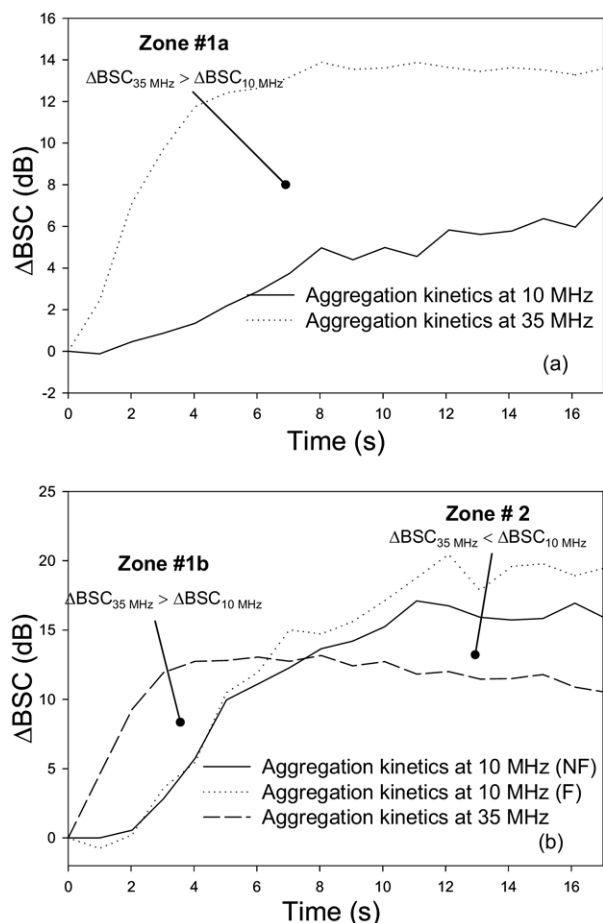


Fig. 12. Aggregation kinetics under steady flow with a step shear rate change from  $100 \text{ s}^{-1}$  to  $2 \text{ s}^{-1}$  (at  $t = 0 \text{ s}$ ) obtained with the 35- and 10-MHz transducers. (a) With normal blood samples (in zone 1a,  $\Delta\text{BSC}$  is higher at 35 MHz during the whole kinetic); (b) with hyperaggregating RBCs (in zone 1b,  $\Delta\text{BSC}$  is higher at 35 MHz and in zone 2  $\Delta\text{BSC}$  is higher at 10 MHz). Note that the 10-MHz nonfocused transducer (NF) gave a similar kinetic than the 10-MHz focused transducer (F).

large RBC aggregates are present (Fontaine and Cloutier 2003; Cloutier *et al.* 2004). Higher  $\Delta\text{BSC}$  at 35 MHz (zones 1a and b) have also been documented (Cloutier *et al.* 2004; Yu and Cloutier 2007), but a clear explanation is still missing.

Cloutier *et al.* (2004) suggested that high-frequency transducers with large bandwidth might have decreased time responses to changes in aggregate sizes and might thus detect more rapidly growths of small RBC clusters than lower frequency transducers. However, this hypothesis alone cannot explain zone 1a of Fig. 12a. Additional suppositions are that low-frequency transducers may have insufficient spatial resolutions to detect changes in small structures (Cloutier and Qin 1997; Huang *et al.* 2005), as it was probably the case for normal TH40 blood. Further investigations are therefore needed to

better understand the higher sensitivity to changes in small aggregate sizes at high frequency.

The results of Fig. 12 are now used to interpret our pulsatile flow observations of Fig. 5. The aggregation kinetic profiles under pulsatile flow had the same tendency as in Fig. 12a, with the maximum backscatter at 35 MHz and no crossing of the 35-MHz and 10-MHz kinetic profiles over time. Therefore, this finding and Figs. 6 and 7 suggest that, for a mean shear rate of  $11.8 \text{ s}^{-1}$ , aggregates of both TH40 and DH40 bloods were not large enough to produce non-Rayleigh effect at 35 MHz under pulsatile flow.

*Effect of the blood sample.* As observed in Figs. 6 and 7, DH40 had significantly greater  $\Delta\text{BSC}_{\text{permanent}}$  than TH40, whatever the ultrasound frequency and stroke rate. The aggregation kinetic slopes were higher for DH40 at 35 MHz at all stroke rates. The higher  $\Delta\text{BSC}_{\text{permanent}}$  suggests that DH40 formed larger aggregates than TH40, whereas the steepest slopes indicate larger growth in size of aggregates over time. These observations are consistent with previous studies on RBCs suspended in large-molecular-weight dextran *vs.* control RBCs in native plasma (Bauersachs *et al.* 1989; Meiselman 1993).

*Effect of the stroke rate.* As reported earlier, the stroke rate applied to the flow did not significantly affect  $\Delta\text{BSC}_{\text{permanent}}$  (Fig. 6,  $p = 0.103$ ) and the aggregation slope (Fig. 7,  $p = 0.675$ ). For any given blood sample, the flow shear rate is recognized as a main determinant of RBC aggregation (Schmid-Schönbein *et al.* 1968), under both steady and pulsatile flows. Because the mean shear rate remained the same in our experiments ( $11.8 \text{ s}^{-1}$ ), whatever the stroke rate as the duty cycle was held fixed at 10%, our findings again support the hypothesis that similar mean aggregate sizes were obtained for a given set of experiments with TH40 or DH40 blood samples.

#### Cyclic variations of echogenicity

According to Table 2, no cyclic variation of BSC could be observed at 10 MHz for 45 BPM and 70 BPM, whatever the blood type. For these cases, the stroke rate did not correspond to the main frequency component of the cyclic variation and the BSC variations could not be related to changes in shear rate. This agrees with previous studies where RBC aggregation and disaggregation were not observed at high stroke rates with a 10-MHz transducer (Cloutier and Shung 1993; Wu and Shung 1996; Lin and Shung 1999; Paeng *et al.* 2001). However, we explain the absence of cyclic variations not because RBCs do not have time to aggregate but because the sensitivity of the 10-MHz transducer to cluster size changes is insufficient. At 35 MHz and 70 BPM, even if cyclic variations were small ( $<0.6 \text{ dB}$ ), spectrograms of BSC revealed consistent pulsations (Fig. 11a and c).

*Effect of the transducer.* We now compare the effect of the transducer at 20 BPM for both blood types. We noted that TH40 had a higher cyclic variation at 35 MHz than at 10 MHz (Fig. 8a, b), but this was not the case for DH40 (Fig. 8c, d). To discuss these results, we again refer to Fig. 12a, b. Note, however, that comparing these steady flow measures to the condition of our pulsatile flow experiments is not straightforward. In Fig. 12, the shear rate was reduced from 100 to  $2 \text{ s}^{-1}$  and observations lasted 17 s. For unsteady flow experiments as in Fig. 5, pulsatility between 100 and  $2 \text{ s}^{-1}$  was maintained for at least 22 s before analyzing BSC of the last 10 cycles. Consequently, each measure of cyclic variation in backscatter experienced a “time history” of  $\sim 22 \text{ s}$  at a mean shear rate of  $11.8 \text{ s}^{-1}$ . Similarities thus exist between conditions of Figs. 5 and 12.

For TH40, we found larger cyclic changes at 35 MHz than at 10 MHz for all stroke rates (Table 2). This can be explained by the fact that small changes in aggregate size between 100 and  $2 \text{ s}^{-1}$  are better detected at 35 MHz (zone 1a of Fig. 12a). Of course, increasing the observation period in permanent regime before analyzing cyclic changes in BSC could have modified conclusions for TH40. For instance, as seen on Fig. 12a, the plateau of  $\Delta\text{BSC}$  was not reached after 17 s at 10 MHz. For DH40, which forms larger aggregates than TH40, the 10-MHz transducer could better sense cyclic variations in permanent regime at 20 BPM (*i.e.*, after more than 22 s of cyclic shearing, which corresponds to zone 2 of Fig. 12b). However, as the stroke rate was increased to 45 and 70 BPM, detecting small changes in large aggregate size was not possible at 10 MHz. In addition to the “time history” in permanent regime, it is clear that the pulsation rate influences the detectability of RBC aggregation and disaggregation at 10 MHz. As introduced earlier, this may be explained by the slower transient time response at 10 MHz (5-MHz bandwidth) than at 35 MHz (17-MHz bandwidth).

#### *Comparison with previous studies on cyclic echogenicity variations*

Cyclic variations in this study were small when compared with previous results obtained with whole porcine blood at 10 MHz (Cloutier and Shung 1993; Wu and Shung 1996; Lin and Shung 1999; Paeng et al. 2001), whereas they cannot quantitatively be compared with De Kroon et al. (1991). First, in the current paper the pulsatile flow was investigated in a Couette system instead of a mock tube flow loop or *in-vivo* conditions. Second, blood echogenicity variations were determined differently from one study to another. De Kroon et al. (1991) quantified them from B-mode grey scale images at 30 MHz, whereas Shung’s group and our group previously examined Doppler power at 10 MHz. Our current

data at 10 and 35 MHz were obtained from RF signals with different SNR and transducer characteristics than previous studies.

## CONCLUSION

Backscattered signals from porcine blood were measured in a pulsatile Couette flow apparatus to compare the effect of the transducer frequency, stroke rate and blood type on echogenicity variations. Two single-element 10-MHz and 35-MHz transducers were used with normal porcine blood and porcine RBCs suspended in dextran to promote hyperaggregation. For both blood types, cyclic variations of echogenicity were observed up to 70 BPM at 35 MHz, whereas cyclic changes were not found at stroke rates higher than 20 BPM at 10 MHz. Unlike what has been proposed in previous studies at a frequency of 10 MHz, RBC aggregation and disaggregation are detectable at a higher frequency of 35 MHz and exist at a physiological stroke rate of 70 BPM. Therefore, the present investigation has shown that high-frequency transducers have a better sensitivity to detect rapid changes in RBC aggregate sizes and can lead to better characterization of RBC aggregation under physiological conditions.

*Acknowledgments*—This work was supported by the Canadian Institutes of Health Research (grant No. MOP-84358). Dr. Cloutier is recipient of the National Scientist award of the Fonds de la Recherche en Santé du Québec (2004-2009). Ms. Nguyen received an undergraduate studentship award from the Natural Sciences and Engineering Research Council of Canada. The authors also acknowledge Les Viandes ULTRA Meats Inc., Saint-Esprit, Quebec, Canada for the supply of blood, and Mr. Ovid Da Silva, Research Support Office, Research Centre, CHUM, for editing this manuscript.

## REFERENCES

- Bauersachs RM, Wenby RB, Meiselman HJ. Determination of specific red blood cell aggregation indices via an automated system. *Clin Hemorheol* 1989;9:1–25.
- Boynard M, Lelievre JC. Size determination of red blood cell aggregates induced by dextran using ultrasound backscattering phenomenon. *Biorheology* 1990;27:39–46.
- Chabanel A, Horellou MH, Conard J, Samama MM. Red blood cell aggregability in patients with a history of leg vein thrombosis: influence of post-thrombotic treatment. *Br J Haematol* 1994;88:174–179.
- Cloutier G, Shung KK. Cyclic variation of Doppler backscattering power from porcine blood in a pulsatile flow model. *IEEE Ultrason Symp* 1991;1301–1304.
- Cloutier G, Shung KK. Study of red cell aggregation in pulsatile flow from ultrasonic Doppler power measurements. *Biorheology* 1993;30:443–461.
- Cloutier G, Qin Z. Ultrasound backscattering from non-aggregating and aggregating erythrocytes—A review. *Biorheology* 1997;54:443–470.
- Cloutier G, Daronat M, Savery D, Garcia D, Durand LG, Foster FS. Non-Gaussian statistics and variations of the ultrasound signal backscattered by blood at frequencies between 10 and 58 MHz. *J Acoust Soc Am* 2004;116:566–577.
- De Kroon MGM, Slager CJ, Gussenhoven WJ, Serruys PW, Roelandt JRTC, Bom N. Cyclic changes of blood echogenicity in high-frequency ultrasound. *Ultrasound Med Biol* 1991;17:723–728.

- Fontaine I, Cloutier G. Modeling the frequency dependence (5-120 MHz) of ultrasound backscattering by red cell aggregates in shear flow at a normal hematocrit. *J Acoust Soc Am* 2003;113:2893-2900.
- Greenleaf JF. *Tissue characterization with ultrasound I*, 1st ed. Boca Raton, FL: CRC Press, 1986:1-245.
- Hayakawa M, Kuzuya F. Effects of Ticlopidine on erythrocyte aggregation in thrombotic disorders. *Angiology* 1991;42:747-753.
- Huang CC, Tsui PH, Wang SH, Chiu CY. Detecting the process of coagulation and clot formation with high frequency ultrasound. *J Med Biol Eng* 2005;25:171-177.
- Le Dévéhat C, Khodabandehlou T, Vimeux M, Aouane F. Diabetes mellitus: Its effects on blood rheological properties and microcirculatory consequences. *Clin Hemorheol* 1996;16:677-683.
- Le Dévéhat C, Khodabandehlou T, Vimeux M. Diabète sucré et fibrinogène: Conséquences hémorhéologiques et microcirculatoires. *J Mal Vasc* 2000;25:53-57.
- Lin YH, Shung KK. Ultrasonic backscattering from porcine whole blood of varying hematocrit and shear rate under pulsatile flow. *Ultrasound Med Biol* 1999;25:1151-1158.
- Meiselman HJ. Red blood cell role in RBC aggregation: 1963-1993 and beyond. *Clin Hemorheol* 1993;13:575-592.
- Neumann FJ, Tillmanns H, Roebruck P, Zimmermann R, Haupt HM, Kübler W. Hemorrhological abnormalities in unstable angina pectoris: A relation independent of risk factor profile and angiographic severity. *Br Heart J* 1989;62:421-428.
- Neumann FJ, Katus HA, Hoberg E, Roebruck P, Braun M, Haupt HM, Yillmanns H, Kübler W. Increased plasma viscosity and erythrocyte aggregation: Indicators of an unfavorable clinical outcome in patients with unstable angina pectoris. *Br Heart J* 1991;66:425-430.
- Paeng DG, Cao PJ, Shung KK. Doppler power variation from porcine blood under steady and pulsatile flow. *Ultrasound Med Biol* 2001;27:1245-1254.
- Paeng DG, Shung KK. Cyclic and radial variation of the Doppler power from porcine whole blood. *IEEE Trans Ultrason Ferroelect Freq Cont* 2003;50:614-622.
- Poggi M, Palareti G, Biagi R, Parenti M, Babini AC, Coccher S. Prolonged very low calory diet in highly obese subjects reduces plasma viscosity and red cell aggregation but not fibrinogen. *Int J Obes* 1994;18:490-496.
- Rouffiac V, Péronneau P, Hadengue A, Barbet A, Delouche P, Dantan P, Lassau N, Levenson J. A new ultrasound principle for characterizing erythrocyte aggregation. *Invest Radiol* 2002;37:413-420.
- Samocha-Bonet D, Lichtenberg D, Tomer A, Deutsch V, Mardi T, Goldin Y, Abu-Abeid S, Shenkerman G, Patshornik H, Shapira I, Berliner S. Enhanced erythrocyte adhesiveness/aggregation in obesity corresponds to low-grade inflammation. *Obes Res* 2003;11:403-407.
- Schmid-Schönbein H, Gaetgens P, Hirsch H. On the shear rate dependence of red cell aggregation in vitro. *J Clin Invest* 1968;47:1447-1454.
- Vayá A, Falcó C, Réganon E, Vila V, Martínez-Sales V, Corella D, Contreras MT, Aznar J. Influence of plasma and erythrocyte factors on red blood cell aggregation in survivors of acute myocardial infarction. *Thromb Haemost* 2004;91:354-359.
- Wang SH, Shung KK. An approach for measuring ultrasonic backscattering from biological tissues with focused transducers. *IEEE Trans Biomed Eng* 1997;44:549-554.
- Weng X, Cloutier G, Pibarot P, Durand LG. Comparison and simulation of different levels of erythrocyte aggregation with pig, horse, sheep, calf, and normal human blood. *Biorheology* 1996;33:365-377.
- Wu SJ, Shung KK. Cyclic variation of Doppler power from whole blood under pulsatile flow. *Ultrasound Med Biol* 1996;22:883-894.
- Yu F, Cloutier G. Experimental ultrasound characterization of red blood cell aggregation using the structure factor size estimator. *J Acoust Soc Am* 2007;122:645-656.